

R-Curve Behaviour of BaTiO₃ due to Stress-Induced Ferroelastic Domain Switching

F. Meschke, A. Kolleck and G. A. Schneider

Technische Universität Hamburg-Harburg, Advanced Ceramics Group, D-21073 Hamburg, Germany

(Received 16 April 1996; revised version received 27 September 1996; accepted 21 October 1996)

Abstract

R-curves of ferroelectric barium titanate have been measured with CT-specimens. Depending on the grain size, the R-curves exhibit an increase from an initial value of 0.5–0.7 MPa√m to a plateau value of 0.7–1.2 MPa√m after a crack length increment of approximately 100–800 μm. The main toughening mechanism is thought to be ferroelastic domain switching leading to the development of a process zone around the crack. The small differences in the initial values of the R-curves are attributed to grain bridging, crack deflection and crack branching associated with large grains. Applying an electric field perpendicular to the specimen plane results in an increased initial fracture toughness and a stronger R-curve behaviour. Time-dependent reorientation of domains in the crack wake causes stress relaxation combined with a strong time dependence of the R-curves. A qualitative process zone model is proposed to explain these effects. © 1997. Published by Elsevier Science Limited.

1 Introduction

Ferroelectrics such as BaTiO₃ or Pb(Zr_xTi_{1-x})O₃ are widely used as capacitor, sensor and actuator materials. For lifetime predictions of components consisting of ferroelectrics the fracture behaviour is most important. Work done by Pohanka *et al.*¹ has shown that barium titanate exhibits a higher strength in the ferroelectric state than in the paraelectric state. An increased toughness has been held to be responsible for this result by Cook *et al.*² who observed that the toughness increases as the temperature is reduced below the Curie temperature. It has been verified using Vickers indentation techniques that poling of ferroelectrics increases the fracture toughness in the poling direction and reduces it in directions perpendicular to poling.^{3–5} Stress-induced domain switching was used to explain, on the one hand, the observed anisotropy

in fracture toughness and, on the other hand, the enhanced toughness in the ferroelectric state compared to the paraelectric state.^{3,4} Rising fracture toughness with increasing indentation load in BiVO₄ was interpreted in terms of R-curve behaviour due to ferroelastic domain switching by Baker *et al.*⁶ Similar results with BaTiO₃ have been presented by Cook *et al.*⁷

In the present study, the fracture resistance curve of barium titanate has been directly measured with compact tension (CT) specimens. The effect of stress relaxation due to domain reorientation as well as the influence of an applied electric field have been examined.

2 Experimental

2.1 Preparation of CT specimens

Samples were prepared from two commercially available barium titanate powders doped with strontium, namely TICON HPB (TAM Ceramics Inc., Niagara Falls, USA) and Alpha 99% – 2 μm (Johnson Matthey GmbH, Karlsruhe, Germany), hereafter referred to as HPB and material B. In order to obtain green bodies, the powders were cold isostatically pressed at 750 MPa. The pressed pieces were sintered at 1250°C for 3 h, and additionally for 27 h in the case of material B in order to enhance grain growth. The samples denoted in the following as B3, B27 and HPB have relative densities of 93, 96 and 95%, respectively.

CT specimens were cut from the plates and ground to dimensions of 24 × 25 × 2 mm³. Two holes of 5 mm diameter were drilled for the fixture of the specimens in the testing device. The specimens were polished with 15 μm and 1 μm diamond paste and thermally etched at 1200°C for 0.5 h.

The testing device is composed of a piezoelectric actuator in the centre and two levers which transfer the load onto the sample.⁸ One lever is equipped with a force sensor in order to detect the force at

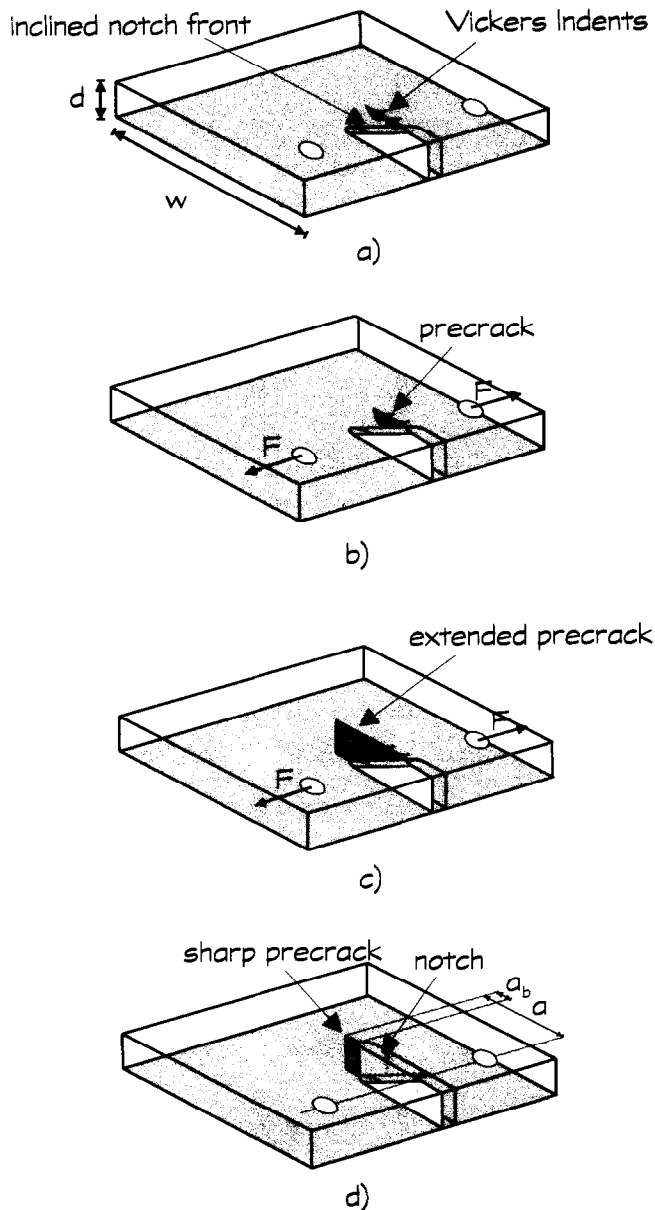


Fig. 1. Geometry of CT specimen with notch, precrack of length a_b and sharp crack of length $a_b + \Delta a$. The overall crack length is a .

the onset of crack growth. The testing device allows in-situ measurement of crack length with an optical microscope.

A special procedure was used to produce a sharp precrack (Fig. 1). First, a notch was cut with its front inclined at 30° to the sample plane. Subsequently, two 5-kg Vickers indents, $250 \mu\text{m}$ apart, were set ahead of the notch front (Fig. 1(a)). After that, the CT specimen was mounted on the testing device and carefully loaded until crack growth and coalescence of the median cracks of the Vickers indents occurred (Fig. 1(b)). Further loading resulted in the formation of a sharp precrack ahead of the inclined notch front (Fig. 1(c)). Before measuring the R-curve, the sample was renotched in order to remove the Vickers indents (Figure 1(d)). The precrack length

a_b ahead of the notch was typically 1 mm in the fine-grained materials and larger than 2 mm in the coarser-grained materials in order to assure that grain-bridging effects are already saturated. Some samples had precrack lengths of a few $100 \mu\text{m}$ in order to study the approach to saturation due to grain bridging. Finally, the CT specimens were annealed at 500°C in order to assure an isotropic domain orientation around the precrack and to relax any residual stresses introduced during the specimen preparation.

The ratio of crack length to specimen width, a/w , was 0.3 initially (Fig. 1). R-curve measurement was stopped as a/w reached 0.5 after crack extension in order to avoid uncertainty in crack resistance due to increasing compliance. An effort was made to keep the crack growth velocity constant at about $0.5 \mu\text{m s}^{-1}$. The fracture toughness was calculated from the applied load P_A , the specimen thickness d and a/w according to eqn (1):⁹

$$K_A = \left(\frac{P_A}{d\sqrt{W}} \right) \left(2 + \frac{a}{w} \right) \left(0.886 + 4.64 \frac{a}{w} - 13.32 \left(\frac{a}{w} \right)^2 + 14.762 \left(\frac{a}{w} \right)^3 - 5.6 \left(\frac{a}{w} \right)^4 \right) \left(1 - \frac{a}{w} \right)^{-1.5} \quad (1)$$

3 Results

3.1 Microstructure and fracture mode

The microstructures and crack paths of the materials examined are shown in Fig. 2. The micrograph of B3 in Fig. 2(a) reveals a fine-grained microstructure with a mean grain size of $0.7 \mu\text{m}$. The microstructures of B27 and HPB shown in Figs 2(b) and 2(c) reveal bimodal grain size distributions. The mean grain sizes for small and large grains are 1.5 and $24 \mu\text{m}$ in the case of B27 and 0.7 and $34 \mu\text{m}$ in the case of HPB, respectively. The volume content of large grains is 18 and 59 vol% for B27 and HPB, respectively. From Fig. 2(a) it becomes apparent that the crack path is 100% intergranular in fine-grained B3. In the B27 and HPB materials, the crack propagates mainly transgranularly through the large grains and intergranularly through the fine-grained sections as becomes evident from the micrographs of the crack wake in Figs 2(b) and 2(c). Crack deflection and crack branching occur within the large grains causing occasional bridge formation. The degree of crack deflection and crack bridging is most pronounced in HPB.

3.2 R-curve behaviour

Figure 3 shows the measured R-curves for the different materials having the long initial crack lengths. The fine-grained B3 material has a short

R-curve starting from 0.5 MPa/m and reaching a plateau fracture toughness of 0.7 MPa/m after a crack extension of 100 μm . The B27 material exhibits a more pronounced R-curve behaviour with an initial fracture toughness of 0.6 MPa/m and a plateau toughness of 0.9 MPa/m which is reached after 300 μm . The coarse-grained HPB reveals further enhanced R-curve behaviour with a transition

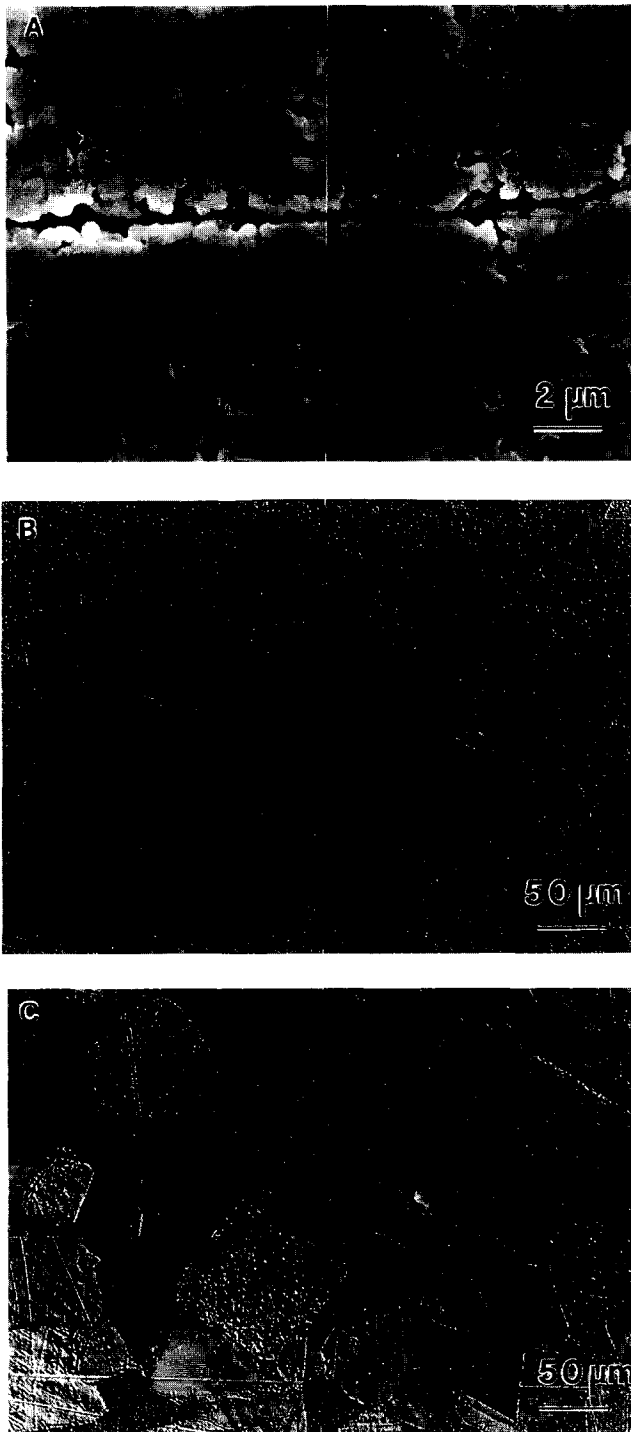


Fig. 2. Microstructure and crack path of the different BaTiO₃ specimens. (a) Fine-grained monomodal grain size distribution in B3 after 3 h sintering with intergranular fracture mode. (b) bimodal grain size distributions with mixed mode fracture in B27 after sintering for 27 h and (c) in HPB after 3 h of sintering.

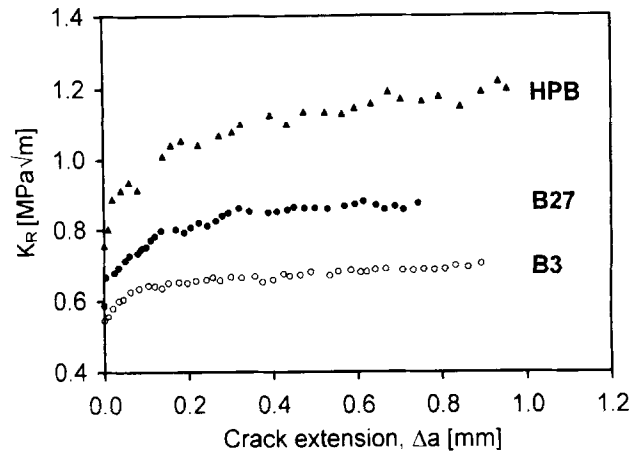


Fig. 3. R-curves of BaTiO₃ materials with different grain size distributions.

regime exceeding 800 μm and initial and plateau values of 0.7 and 1.3 MPa/m, respectively.

3.3 R-curve behaviour after room temperature ageing

When crack advance was stopped by unloading and the CT specimen was reloaded after a certain time, the fracture toughness at crack growth onset was considerably lower than it had been before unloading. As shown in Fig. 4a, it drops down by 10, 20 and 50% as observed in HPB after 1, 2 and 30 min. After unloading of 18 h, the initial fracture toughness was equal to that of the primary R-curve as shown in Fig. 4(b) for a HPB sample which had a slightly reduced amount of large grains.

3.4 R-curve behaviour after poling and the application of an electrical field

After annealing for 4 h at 500°C, the R-curve of HPB was measured under an applied electric field of 500 V mm⁻¹ perpendicular to the specimen plane. For this purpose a thin gold layer was sputtered to form electrodes on two opposing surfaces. The result shown in Fig. 5 clearly reveals an increase of the initial fracture toughness from 0.75 MPa/m to 1 MPa/m and a shorter crack extension to reach the plateau value of the R-curve in comparison to an unpoled specimen without the application of an electrical field.

4 Discussion

The R-curve behaviour of ferroelectric BaTiO₃ has been established with CT specimens for three materials which mainly differ in the volume content of large grains dispersed in a fine-grained matrix. The effect of porosity is of minor importance. It probably shifts the initial fracture toughness of B3 to lower values but should have no effect on the domain switching. In the following

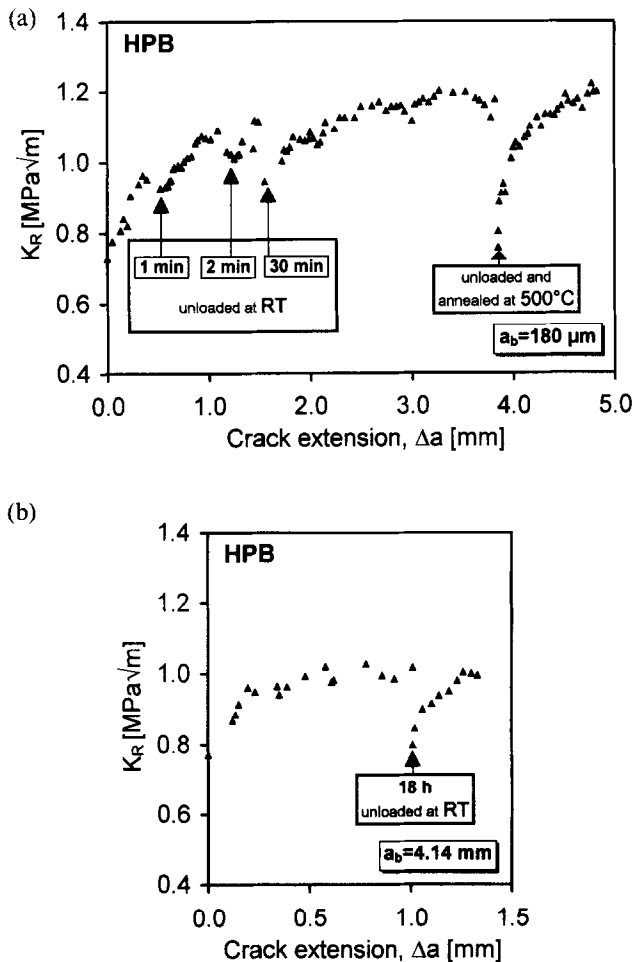


Fig. 4. Loss in fracture toughness after unloading for different times at room temperature and 'restarted' R-curve behaviour after reloading. (a) Unloading times: 1 min, 2 min, 30 min. (b) Unloading time: 18 h. The slightly lower plateau value of this R-curve is due to a somewhat smaller amount of large single grains in this sample from a different batch.

we discuss in detail the contribution of crack branching, deflection and bridging and ferroelastic domain switching to toughening. The most important toughening mechanism is thought to be ferroelastic domain switching as has been proposed by various researchers.¹⁻⁷

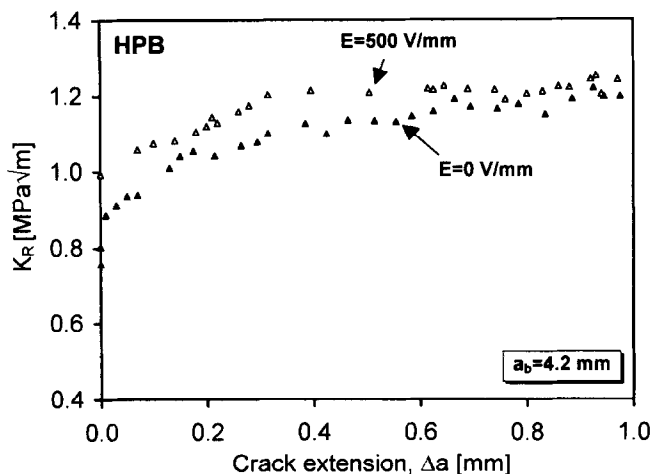


Fig. 5. R-curve comparison in HPB without and with applied electric field of 500 V mm^{-1} parallel to the crack front.

4.1. R-curve behaviour due to domain switching

Domain switching increases toughness as has been outlined by Mehta *et al.*⁴ In order to explain the R-curve behaviour in a qualitative way, we use a model similar to that for transformation toughening in zirconia ceramics containing metastable tetragonal phase. In zirconia, the tetragonal/monoclinic phase transformation is stress-induced within a process zone around the crack tip. The volumetric dilation of 5 vol%, associated with the transformation results in compressive stresses. When the crack extends, these compressive stresses act on the crack wake and cause shielding of the crack tip from the applied load. The pronounced R-curve behaviour of zirconia is due to increasing compressive stresses in the crack wake with increasing crack length.

Similarly, in ferroelectrics like BaTiO_3 , the toughening is related to the stress-induced domain switching process near the crack tip due to the high tensile stresses. The polar rotation of domains by 90° causes a strain mismatch of up to 1% ($(c-a)/a=0.01$). Due to the tetragonal anisotropy, compressive stresses are caused. These compressive stresses are created perpendicular to the crack plane because of the preferred orientation of the c-axis of the tetragonal BaTiO_3 in this direction. When the crack extends, compressive stresses associated with the orientation of the polar axis of the domains mainly normal to the crack surface act in the crack wake and cause shielding of the crack tip from the applied load as in the case of zirconia. The length of the crack wake where the compressive stresses act becomes longer on crack extension and ΔK_w rises to a maximum value ΔK_w^{\max} where the plateau value of the R-curve is reached. Similar to transformation toughening, ΔK_w should be a function of the zone width, h , and the shape of the frontal zone. The R-curves exhibit a ΔK_w^{\max} of up to $0.5 \text{ MPa}\sqrt{\text{m}}$, which, when compared to the intrinsic toughness of $0.7 \text{ MPa}\sqrt{\text{m}}$, gives an enhancement in fracture toughness of 70%. This is comparable to the contribution of transformation toughening in zirconia or zirconia-toughened ceramics.¹¹ In addition to the compressive stresses, tensile stresses are present parallel to the crack plane. However, the tensile stresses parallel to the crack plane are, in a first approximation, not of importance for the stress intensity factor at the crack tip.

The driving force for switching is the minimisation of the elastic free energy within the frontal zone.³ In contrast to the tetragonal/monoclinic phase transformation in ZrO_2 , the volume change during switching is zero and only shear stresses will initiate the domain switching. The consequence is a different zone shape. No information

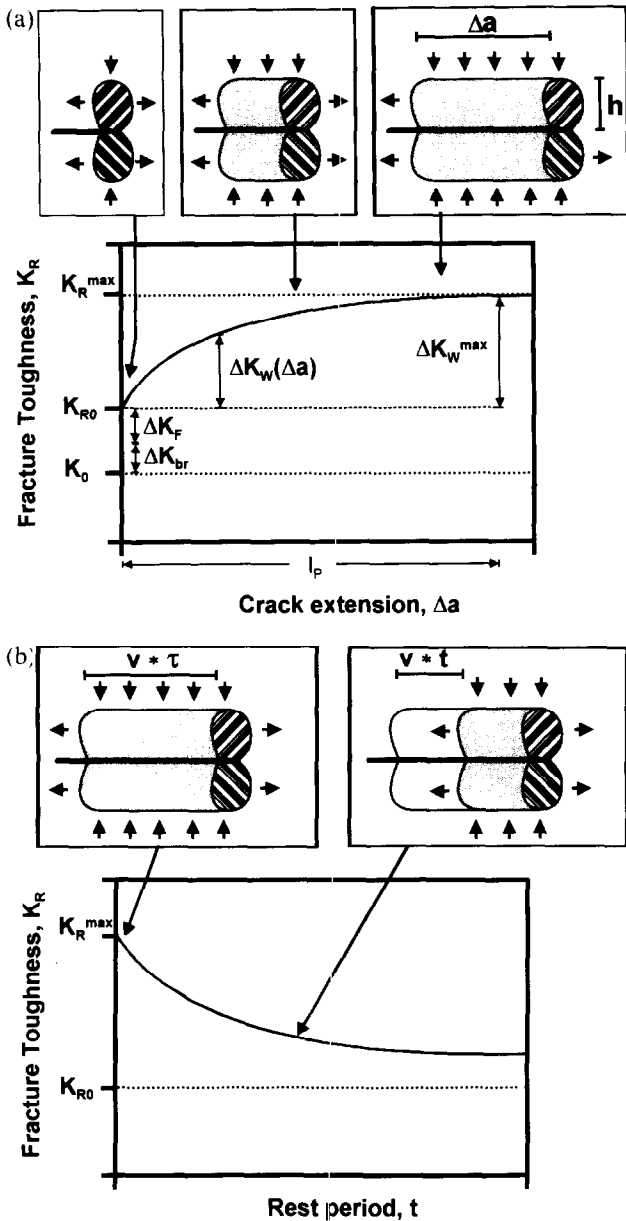


Fig. 6. Process zone model for BaTiO₃. (a) Fracture toughness increase ΔK_F due to the frontal zone and ΔK_W due to the compressive stresses in the crack wake. (b) Domain back switching during unloading with associated fracture toughness loss of the material.

is currently available on the real shape of the frontal process zone arising in the remote stress field in ferroelectrics. A dog-bone shape similar to that observed in the case of yielding in metals might be a good approximation (Fig. 6(a)) because the shear component of the stress field should similarly initiate the switching process. The dog-bone frontal zone by itself might enhance the toughness by a fixed amount ΔK_F as in the case of transformation toughening.¹¹ The R-curve can then be described by

$$K_R(\Delta a) = K_0 + \Delta K_F + \Delta K_W(\Delta a) \quad (2)$$

with K_0 giving the intrinsic toughness of the material.

4.2 Grain-size dependence

It is observed that an increasing grain size, or more precisely, an increasing number of large grains present in the fine-grained microstructure, leads to an increase in the initial value of the R-curve. Additionally, it leads to a more pronounced R-curve as expressed by a higher K_R^{max} and a longer zone length l_p to reach the plateau value (Fig. 3).

Because the R-curves were measured in annealed samples with long precracks, we can draw the following conclusions. Due to the annealing at 500°C, compressive stresses in the crack wake are relaxed and cannot contribute to the measured initial toughness of the R-curve. Only toughening from the process zone as well as crack deflection inside the transgranularly fractured large grains (Fig. 2(b)), crack bridging and crack branching at large grains (Fig. 2(c)) increases the initial fracture toughness K_{R0} of the R-curve

$$K_{R0} = K_0 + \Delta K_F + \Delta K_{br} \quad (3)$$

ΔK_{br} stands for the contributions of crack deflection, bridging and branching. ΔK_{br} is assessed to be constant because the precrack is very long (up to 4 mm) and the effects are saturated. It follows that the plateau value of the R-curve can be described as (see Fig. 6(a))

$$K_R^{max} = K_{R0} + \Delta K_W^{max} \quad (4)$$

In order to explain the increase of ΔK_W^{max} with increasing grain size, we have to consider the zone-size dependence of ΔK_W^{max} . In analogy to transformation toughening, ΔK_W^{max} can be calculated from¹¹

$$\Delta K_W^{max} = \alpha \sqrt{h} \epsilon_T \quad (5)$$

where α is a constant including Young's modulus, ϵ_T is related to $(c-a)/a$ and corresponds to the transformation strain. h denotes the width of the process zone and is given according to Becher and Swain¹⁶ by

$$h = A \left(\frac{K_{R0}}{\sigma_S^c} \right)^2 \quad (6)$$

In eqn (6) A is a constant and σ_S^c is the critical stress for domain switching. Increasing the grain size results in an increase of ΔK_{br} , and according to eqn (3), in an enhanced K_{R0} . From eqns (5) and (6) this results in an increase in h , and therefore, a higher ΔK_W^{max} .

However, for the explanation of the higher ΔK_W^{max} the dependence of σ_S^c on grain size has also to be taken into account. According to Suo,¹² the energy release rate G for a band of an a -domain

of thickness b , advancing in an infinite c -domain is, in the absence of an electric field:

$$G = 2\gamma_s\sigma_s b \quad (7)$$

with $\gamma_s = (c-a)/a$. The energy is consumed by creating domain walls with surface energy Γ . Therefore the critical shear stress σ_s^c is determined by $G=2\Gamma$ leading to:

$$\sigma_s^c = \frac{\Gamma}{\gamma_s b} \quad (8)$$

It is well-known from the work of Arlt¹³ that domain thickness decreases with decreasing grain size which results in an increasing σ_s^c according to eqn (8). Earlier work by Hennings has shown that, for grain sizes below 0.7 μm , the critical stress is such that the domains cannot be switched electrically.¹⁴ Detailed information is, however, very limited. Nevertheless, it can be concluded that the decreasing σ_s^c for increasing grain size results in larger zone widths h according to eqn (5).

The final conclusion is that both the increase of ΔK_{br} and the decrease of σ_s^c with increasing grain size leads to a larger process zone width h , and therefore, to a higher plateau value of the R-curve. In addition, it is known for transformation-toughened ceramics that the crack extension, l_p , to reach the plateau value of the R-curve scales with the zone width according to $l_p \approx 5h$.¹⁵ Assuming a similar relationship for toughening by switching leads to the conclusion that l_p should increase with increasing grain size as observed.

4.3 Time-dependence

Another important observation, which is quite different from observations with zirconia-toughened ceramics, is that after a certain relaxation time nearly all domains can switch back in the crack wake. This implies that, depending on the relaxation time, a limited zone length persists. The actual zone length l can be determined from the relaxation time τ , the crack velocity v and the time t of crack growth:

$$l(t) = \int_{t-\tau}^t v(t) dt, \text{ for } \tau < t \quad (9a)$$

$$l(t) = \int_0^t v(t) dt, \text{ for } \tau < t \quad (9b)$$

For a constant crack velocity v_0 the result simplifies to

$$l = v_0 t, \text{ for } \tau > t \quad (10)$$

$$l = v_0 \tau, \text{ for } \tau < t \quad (11)$$

The drop in fracture toughness when the R-curve measurement is interrupted is due to the diminished zone length behind the crack tip after back switching has occurred. As indicated in our relaxation model, Fig. 6(b), the associated shielding is reduced. The loss in fracture toughness after a certain unloading time t_s is determined basically by the relaxation time τ . If we assume an exponential decay, $\exp(-t/\tau)$, the relaxation time can be roughly estimated from Fig. 4(c) giving a value of approx 30 min. Using this value to calculate the maximum process zone length $v_0 \tau$ gives 900 μm for HPB ($v = 0.5 \mu\text{m/s}$ according to Section 2.1), which corresponds well with the zone length l_p of approx 800 μm , where the R-curve saturates.

4.4 Effect of an electric field

As shown in Fig. 5, the application of an electric field parallel to the crack front increases K_{R0} . We assume that ΔK_{br} is not strongly influenced by the electric field and therefore according to eqn (3) it must be concluded that ΔK_F increased.

The R-curve measurement of the poled sample under the application of an applied electric field delivers a strong hint that the process zone ahead of the crack tip already increases the initial fracture toughness. Due to the orientation of the electric field parallel to the crack front, the volume fraction of switchable domains increases in comparison to the case without electric field and an increase in initial fracture toughness results. However, it is surprising that the plateau value of the R-curve, K_R^{max} , is not significantly enhanced. One explanation could be that the electric field, which is parallel to the crack surface, delivers an additional driving force to switch back the domains. A consequence would be a smaller relaxation time τ and therefore a smaller zone length l_p .

5 Conclusions

It has been shown that BaTiO₃ has a rising fracture resistance curve. The shape of the R-curve changes with grain size in such a manner that, with coarser grain structures, the plateau value as well as the crack extension associated with the rising part of the R-curve are shifted to higher values. This effect is explained by two mechanisms:

1. Fine-grained BaTiO₃ has intergranular fracture with no visible crack deflection or bridging processes. For coarser-grained BaTiO₃, crack bridging, crack deflection and crack branching are observed at large grains, resulting in an increasing fracture toughness.
- 2(a). A process zone develops which is caused by domain switching in a frontal zone

around the crack tip. The frontal zone as well as the compressive zone in the crack wake which develops during crack advance contribute to the R-curve behaviour. The width h of the process zone increases for coarser-grained materials due to mechanical bridging and a decreasing critical shear stress σ_{ξ}^c for domain switching. In analogy to the martensitic phase transformation in ZrO₂-ceramics, we assume that the process zone length l_p over which a saturation in toughening is reached, is proportional to the zone width. Therefore, in the case of coarse BaTiO₃, the rising part of the R-curve will be longer.

- (b) Domain switching induced by the high stresses at the crack tip is completely reversible with a characteristic relaxation time depending on grain size. Due to the reversibility, the R-curve behaviour is time-dependent.
- (c) A higher volume content of switching domains produced by application of an external electric field increases the initial fracture toughness. Because this effect is not observed in ZrO₂-toughened ceramics we conclude that the shape of the process zone around the crack tip is mostly determined by the deviatoric part of the stress tensor.

We assume that these effects are of general importance for piezoelectric ceramics, and in particular for PZT.

Acknowledgement

The authors thank S. Lathabai for helpful discussions and advice.

References

1. Pohanka, R. C., Freiman, S. W. and Bender, B. A., Effect of the phase transformation on the fracture behavior of BaTiO₃. *J. Am. Ceram. Soc.*, 1978, **61**(1–2), 72–75.
2. Cook, R. F., Freiman, S. W., Lawn, B. R. and Pohanka, R. C., Fracture of ferroelectric ceramics. *Ferroelectrics*, 1983, **50**, 267–272.
3. Pisarenko, G. G., Chusko, V. M. and Kovalev S. V., Anisotropy of fracture toughness of piezoelectric ceramics. *J. Am. Ceram. Soc.*, 1985, **68**(5), 259–265.
4. Mehta, K. and Virkar, A. V., Fracture mechanics in ferroelectric-ferroelastic lead zirconate titanate (Zr:Ti = 0.54:0.46) ceramics. *J. Am. Ceram. Soc.*, 1990, **73**(3), 567–474.
5. Zhang, Z. and Rash, R., Influence of grain size on ferroelastic toughening and piezoelectric behavior of lead zirconate titanate. *J. Am. Ceram. Soc.*, 1995, **78**(12), 3363–3388.
6. Baker, T. L., Faber, K. T. and Readey, D. W., Ferroelastic toughening in bismuth vanadate. *J. Am. Ceram. Soc.*, 1991, **74**(7), 1619–1623.
7. Cook, R. F., Lawn, B. R. and Fairbanks, C. J., Microstructure–strength properties in ceramics I: Effect of crack size on toughness. *J. Am. Ceram. Soc.*, 1985, **68**(11), 604–615.
8. Rödel, J., Kelly, J. F., Stoudt, M. R. and Bennison, S. J., A loading device for fracture testing of compact tension specimen in the SEM. *Scanning Microscopy*, 1991, **5**(1), 29–35.
9. ASTM E 399-83, Standard Test Method for Plane-Strain Fracture Toughness of Metallic Materials. In *1987 ASTM Annual Book of Standards*, Vol. 3.01, American Society for Testing and Materials, Philadelphia, PA, 1987, pp. 680–715.
10. Evans, A. G. and Cannon, R. M., Toughening of brittle solids by martensitic transformations. *Acta Metall.*, 1986, **34**, 761–800.
11. Green, D. J., Hannink, R. H. J. and Swain, M. V. In *Transformation Toughening of Ceramics*. CRC Press, Boca Raton, Florida, 1989.
12. Suo, Z., Mechanics concepts for failure in ferroelectric ceramics. In *Smart Structures and Materials*, ed. A. V. Srinivasan. ASME, New York, 1991, pp. 1–6.
13. Arlt, G., Review: Twinning in ferroelectric and ferroelastic ceramics: Stress relief. *J. Mater. Sci.* 1990, **25**, 2655–2666.
14. Hennings, D., Barium titanate ceramic materials for dielectric use. *Int. J. High Technol. Ceram.*, 1987, **3**, 91–111.
15. Evans, A. G., Toughening mechanisms in zirconia alloys. In *Science and Technology of Zirconia II, Advances in Ceramics*, **12**, ed. M. Rühle, N. Claussen & A. H. Heuer. The American Ceramic Society, Columbus, Ohio, 1984, pp. 382–390.
16. Becher, P. F. and Swain, M. V., Grain-size-dependent transformation behavior in polycrystalline tetragonal zirconia. *J. Am. Ceram. Soc.*, 1992, **75**(3), 493–502.